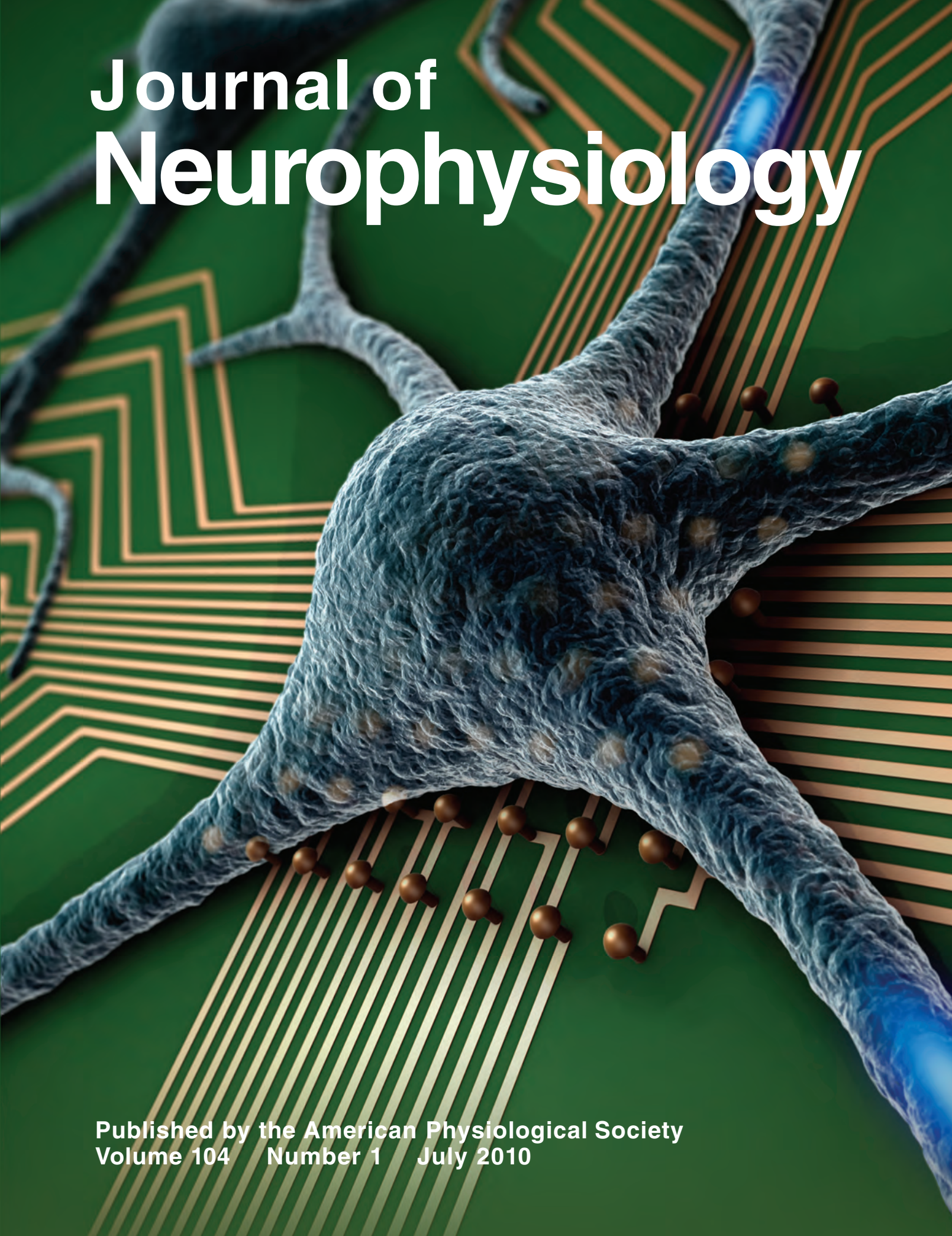

Published by the American Physiological Society
Volume 104 Number 1 July 2010

J Neurophysiol 104: 559–568, 2010.
First published April 28, 2010; doi:10.1152/jn.00265.2010.

Long-Term, Multisite, Parallel, In-Cell Recording and Stimulation by an Array of Extracellular Microelectrodes

Aviad Hai,[1] Joseph Shappir,[2] and Micha E. Spira[1]
[1]*The Life Sciences Institute,* [2]*School of Engineering. The Hebrew University of Jerusalem, Jerusalem, Israel*

Submitted 15 March 2010; accepted in final form 22 April 2010

Hai A, Shappir J, Spira ME. Long-term, multisite, parallel, in-cell recording and stimulation by an array of extracellular microelectrodes. *J Neurophysiol* 104: 559–568, 2010. First published April 28, 2010; doi:10.1152/jn.00265.2010. Here we report on the development of a novel neuroelectronic interface consisting of an array of noninvasive gold-mushroom-shaped microelectrodes (gMμEs) that practically provide intracellular recordings and stimulation of many individual neurons, while the electrodes maintain an extracellular position. The development of this interface allows simultaneous, multisite, long-term recordings of action potentials and subthreshold potentials with matching quality and signal-to-noise ratio of conventional intracellular sharp glass microelectrodes or patch electrodes. We refer to the novel approach as "in-cell recording and stimulation by extracellular electrodes" to differentiate it from the classical intracellular recording and stimulation methods. This novel technique is expected to revolutionize the analysis of neuronal networks in relations to learning, information storage and can be used to develop novel drugs as well as high fidelity neural prosthetics and brain-machine systems.

INTRODUCTION

The development of intracellular recordings and stimulation technologies were hallmark developments that enabled a generation of scientists to decipher the "language" by which neurons transmit information and communicate. With excellent signal-to-noise ratio, sharp-intracellular microelectrodes and patch electrodes enabled researchers to resolve subthreshold miniature and synaptic potentials as well as to analyze the generation of action potentials. In addition, intracellular current injections through these electrodes serve to repeatedly stimulate the neurons as well as to extract essential biophysical parameters such input resistance, membrane capacitance, and analyze synaptic properties (e.g., reversal potentials). Nevertheless the use of sharp or patch microelectrodes for parallel recording or stimulation from many neurons is technically limited as the micromanipulation of the electrode tips toward target cells requires the use of rather bulky micromanipulators (but see Berger et al. 2009; Le Be and Markram 2006). In addition, the duration of intracellular recording and stimulation sessions by these electrode is limited as with time, mechanical instabilities damage the plasma membrane, or in the case of the patch electrodes, perfusion of the cytoplasm alters the intracellular composition of the cells (Sakmann and Neher 1984; but see Akaike and Harata 1994). In contrast, the use of noninvasive extracellular microelectrode arrays enables investigators to record and stimulate large populations of excitable cells for days and months without inflicting mechanical damages to the cell plasma membrane (Berdondini et al. 2009; Hochberg et al. 2006; Hutzler et al. 2006; Rubehn et al. 2009; Shahaf et al. 2008). The most severe disadvantage of extracellular recording electrodes is their low signal-to-noise ratio. Therefore the use of extracellular electrodes is limited to recordings of field potentials generated by action potentials (Fromherz 2006; Fromherz et al. 1991). Only in rare cases can synchronized synaptic potentials in highly ordered neuronal networks be picked up by extracellular electrodes (Neves et al. 2008). Single excitatory or inhibitory subthreshold synaptic potentials or membrane voltage oscillations cannot be detected by existing extracellular electrode technology. These shortcomings limit the use of extracellular recordings to the analysis of spike patterns and firing rates (Fee et al. 1996; Shoham et al. 2003). Alternative methods to "noninvasively" record activity from neuronal networks by the use of voltage-sensitive dyes, electroencephalography (EcoG), or even functional magnetic resonance imaging (fMRI) provide integrated electrical activity from hundreds of cells and suffer from low spatial resolution, toxicity, or reflect indirect manifestations of neuronal electrical activity such as oxygen consumption from blood capillaries.

Experimental and theoretical considerations (Cohen et al. 2008; Fromherz 2006; Jenkner and Fromherz 1997) revealed that the limiting factor for effective electrical recordings of neuronal activities by the sensing pads of extracellular electrodes are the width and surface area of the cleft formed between the cell plasma membrane and the sensing pads, which determines the magnitude of the so called seal resistance (R_{seal}).

In recent years, we began to develop a new approach to better interface neurons and lithographed sensing pads (Hai et al. 2009a,b, 2010; Spira et al. 2007). To that end, we selected what we believed to be a suitable three-dimensional (3D) geometry and dimensions for the microelectrodes (μE) that protrude from the glass substrate and used a specific peptide to functionalize the microelectrodes such that it will activate conserved cell biological mechanisms to generate intimate contact between the neurons and the μE. The 3D μE that we designed to facilitate the formation of an intimate contact is a gold mushroom-shaped microelectrode [gMμE, also termed FGSE—functionalized gold-spine electrode— in a previous brief communication (Hai et al. 2010)], which protrudes from the substrate to a height of 1–1.5 μm (Fig. 1). To "replace" the classical approach of pushing microelectrodes into the cell, we used a peptide that induces, at the cell-μE point of contact, phagocytotic activity (a conserved cell biological mechanism for the internalization of particles) (Stuart and Ezekowitz 2005). The peptide that generates "phagocytosis" of the gMμE by the neuron is a cysteine (C) terminated peptide with a number of RGD repeats (R = arginine, G =

Address for reprint requests and other correspondence: M. E. Spira, The Life Sciences Institute, The Hebrew University of Jerusalem, Jerusalem, Israel (E-mail: spira@cc.huji.ac.il).

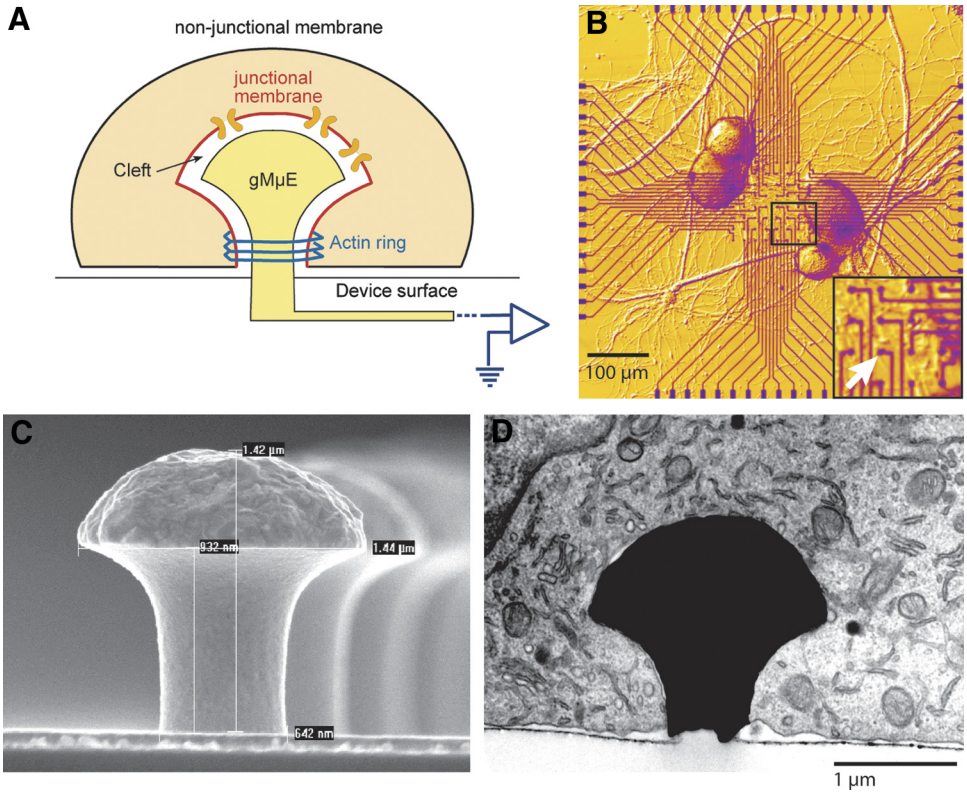

FIG. 1. The in-cell recording and stimulation configuration. *A*: a schema depicting a gold mushroom-shaped microelectrode (gMμE). The gMμE is engulfed by a neuron (orange). The electrode engulfment yields high coupling between the cell and electrode based on 3 principles: narrow cleft between the cell and the electrode yielding a high seal resistance, formation of an actin ring, and accumulation of voltage independent ion channels at the junctional membrane (red, membrane in contact with the gMμE). *B*: phase-contrast image showing *Aplysia* neurons grown on a gMμE array (image selected to emphasize array). *Inset*: closeup of the array, a gMμE is shown at the tip of each electrode (white arrowhead). *C*: scanning electron microscope image of a gMμE. *D*: transmission electron micrograph of a PC12 cell engulfing a gMμE.

glycine, D = aspartic acid), and a long decalysine (K_{10}) spacer, which is covalently linked to the gMμE. This peptide was referred to as the engulfment promoting peptide (EPP): CKKKKKKKKKPRGDMPRGDMPRGDMPRGDM. Using electron microscopy (Hai et al. 2009a; Spira et al. 2007), we established that the neuron-gMμE formed a reduced cleft width and increased contact area. Nevertheless the gMμE clearly maintains an extracellular position in respect to the neuron's plasma membrane. Live confocal microscope imaging of neurons grown on gMμE-based matrixes revealed that the engulfment of the gMμE is associated with restructuring of the actin cytoskeleton to form an actin ring around the stalk of the gMμE (Hai et al. 2009b).

Using an electrophysiological approach, we extend here the characterization of the neuron-gMμE interface by analyzing both the recording and stimulation capabilities of gMμE based microelectrode array (MEA), demonstrate long term use of the gMμEs, and provide a model to explain the nature of the unprecedented bidirectional neuron-electrode coupling. We show that arrays of gMμEs act as an extracellular, microelectrode array system that provides "in-cell" recordings of subthreshold synaptic potentials and action potentials, from individual neurons with excellent signal-to-noise ratio as well as allowing for effective stimulation.

We refer to the novel approach as in-cell recording and stimulation by extracellular electrodes to differentiate it from the classical intracellular recording and stimulation methods in which the electrode tips are forced through the plasma membrane to form direct contact with the cytosol (as is the case of sharp intracellular electrodes) or the breaking-off of the cell's plasma membrane forming direct contact between the cytosol and the patch electrode interior solution (as is the case of patch electrodes) (Sakmann and Neher 1984).

METHODS

Fabrication of gMμE microelectrode arrays

Arrays of gMμE electrodes for electrical measurements were prepared on glass wafers as previously described (Hai et al. 2009a). Briefly, wafers were coated with a Ti (10–15 nm)/Au (45–65 nm) layer by way of evaporation and spin-coated with photoresist S-1813 (4000 RPM) baked for 30 min (90°C) after which a first photolithographic process was performed followed by Au/Ti wet etch to define the microelectrode array. Next a second lithographic step with thick photoresist was performed to open holes for the deposition of the gMμE stalks as well as the contact pads. Gold mushrooms (along with thick metal on the contact pads) were grown by way of electroplating. Next a layer of silicon-oxide (~3,000 Å) was deposited by chemical vapor deposition processing. A third layer of photoresist was then applied. A third lithographic step was used to expose the contact pads and the heads of the gold mushrooms followed by wet oxide etch to selectively remove the oxide from the contact pads and the mushroom heads. Wafers were then sawed and underwent manual bonding to 62-pad printed circuit boards to which 21 mm glass rings were attached to create a recording bath chamber for the culturing medium.

Surface functionalization

Functionalization by the cysteine (C) terminated engulfment promoting peptide (EPP): CKKKKKKKKKK-PRGDMPRGDMPRGDMPRGDM (MW 3630 g/mol) with a number of RGD repeats and a decalysine $(K)_{10}$ spacer was done as follows: gold surface functionalization was done by direct application of the peptide onto the surface (1 mM in phosphate buffer saline at room temperature). The glass surface in between the gold mushrooms underwent surface functionalization using 3-aminopropyltrimethoxysilane (APTMS, Aldrich, 1% in MeOH, 10 min in room temperature) to introduce terminal amine groups to the glass surface. Samples were then washed with MeOH to remove uncoupled APTMS. The protein immobilization linker 4-maleimidobutyric acid sulfo-*N*-succinimidyl ester (sGMBS, Sigma, 0.5%

in PBS) was then applied to the surface and washed with PBS after 40 min at room temperature. EPP peptide was then applied to the surface and left for 24 h in which the cysteinic thiol residue reacts with the maleimido part of the anchored linker. Samples were then washed with PBS.

Cell cultures

Neurons from the buccal ganglia of *Aplysia californica* were isolated and maintained in culture as previously described (Spira et al. 1996). Briefly, juvenile *Aplysia* (1–10 g) supplied from the University of Miami, National Resource for Aplysia, Miami, FL, were anesthetized by injecting isotonic $MgCl_2$ solution (380 mM) into the animal's body cavity. Ganglia were dissected and incubated in L-15 supplemented for marine species (ms L-15) containing 1% protease (type IX, Sigma-Aldrich, Rehovot, Israel) at 34°C for 1.5–2.5 h. Following the protease treatment, the ganglia were desheathed. Individual neurons were manually pulled out along with their original axons with the aid of a sharp glass microelectrode and plated on the devices. Plated *Aplysia* neurons survive in culture for over a month, extend neurites, and form chemical and electrical synapses (Bailey and Kandel 2008). For the present study, neurons plated on the gMμE devices were cultured for 48–96 h at 24°C and then used for the electrophysiological experiments. For the current study, the gMμE devices were used once.

Electrophysiology

Conventional intracellular recording and stimulation of cultured *Aplysia* neurons were used as previously described (Hai et al. 2009a). The microelectrodes were pulled from 1.5/1.02 mm borosilicate glass tubes with filaments, and filled with 2 M KCl. Electrode resistance ranged between 4 and 10 MΩ. For intracellular recording and stimulation, the microelectrode tip was inserted into the cell body.

Recordings were made from the 62 chemically functionalized gMμEs using the Multi Channel Systems (Reutlingen, Germany) AC amplifier (MEA-1060-Inv-BC) with frequency limits of 1–10,000 Hz and a gain of 110–1,100. The experimental data shown (Figs. 2–6) are of raw, unprocessed recordings. Stimulations were done using the STG 1001 (Multi Channel Systems). All stimulations were bipolar in reference to the gMμE/glass-micropipette ground.

Computer simulation and off-line deconvolution

Computer simulations and deconvolutions were done using PSPICE (OrCAD). For the simulations, the parameters used were: *1*) the nonjunctional membrane resistance (R_{nj}), which was measured in a large number of neurons with an average value of 25 MΩ in accordance with the experimentally measured R_{in}. *2*) Junctional membrane resistance (R_j): estimating gMμE area to be $\sim$14 μm^2 and multiplying the total input resistance (R_{in}) with the ratio between the surface area of the neuron and the surface area of the gMμE, we estimated R_j to be $\sim$100 GΩ. *3*) The nonjunctional membrane capacitance C_{nj} equals the total membrane capacitance C_m (according to the same considerations of area ratio) and was set to 600 pF as measured previously in our laboratory (Ashery et al. 1996). *4*) The estimated junctional membrane capacitance (C_j) is calculated as the total membrane capacitance (C_m) divided by the ratio between the surface area of the cell and the surface area of the gMμE and was taken as 0.1 pF. (5) The gMμE resistance ($R_{gM\mu E}$) in solution was estimated to be 1,000 GΩ in accordance with the measured resistance of gold electrodes in physiological solution (McAdams et al. 2006) normalized by the gMμE surface area. *6*) The capacitance of the gMμE in solution is estimated by taking the specific capacitance of gold electrical double layer to be $\sim$50 $\mu F/cm^2$ (Mirsky et al. 1997) multiplied by the surface area of the gMμE and ranges between 0.5 and 25 pF. *7*) The amplifier input capacitance is 8 pF (Multi Channel Systems).

For the simulations, we have replicated action potentials by taking the glass-micropipette recordings from the experiments and feeding it off-line to the simulator. The coupling coefficients were calculated as an algebraic scaling factor between the amplitudes of simulated gMμE and glass micropipette signals.

For the off-line deconvolution, the experimentally recorded signals were used as input to a negative capacitance compensation circuit using the same gMμE and amplifier parameters of the simulations (no iterations or algorithms were used).

Parts of the results presented here were published in a form of brief communication (Hai et al. 2010).

RESULTS

In-cell recording by gold mushroom-shaped extracellular microelectrodes—phenomenology

The experiment of Fig. 2 depicts the main features of the "in-cell recording" configuration. For the experiment, an *Aplysia* neuron was cultured on an array of 62 gMμE functionalized with the engulfment promoting peptide (EPP) for 2 days. A sharp glass microelectrode (coupled through a conventional DC amplifier) for both current injection and voltage recording was inserted into the soma of the neurons. Depolarizing current pulses of varying intensities (Fig. 2*A, i* and *ii,* black) were delivered by the intracellular electrode and generated a single or a train of action potentials recorded by the same glass microelectrode (Fig. 2, red) and the gMμEs (Fig. 2, blue, coupled through an AC amplifier, see following text). The action potentials recorded by the gMμEs were monophasic, positive potentials that resemble in shape the intracellularly recorded action potentials (APs, Fig. 2, *A* and *B*). In the experiment of Fig. 2, APs were recorded by 6 gMμEs that resided beneath the stimulated neuron's cell body (Fig. 2, *e1–e6,* blue). The amplitudes of the raw APs recorded by *e1–e5* were in the range of 5–10 mV, while those recorded by *e6* were $<$1 mV. Interestingly, even the small APs of *e6* were positive monophasic potentials (Fig. 2*B*). Other gMμEs not residing beneath the neuron's cell body did not record any signals (*e7, e8*). This fact demonstrates the lack of cross-talk artifacts from neighboring microelectrodes. Using the same configuration, we recorded in other experiments monophasic action potentials with amplitudes of $\leq$25 mV. As discussed in the following text, the amplitude and shape of APs recorded by gMμEs reflect differences in the electrical coupling between the neuron and individual gMμEs and the impedance of the gMμEs.

Hyperpolarizing pulses of increased amplitude delivered by the intracellular microelectrode generated membrane hyperpolarization (Fig. 2, *iii* and *iv,* red) that were picked up also by gMμEs *e1–e6.* This clearly demonstrates that the interface formed between the neuron and the gMμE generates electrical coupling sufficient to enable parallel multiple site recordings of APs and subthreshold potentials. It is important to note that the impedance of the gMμEs and the AC amplifiers used for the recording by the gMμE filter the APs and thus alter their shape (compare the shapes of the square calibration pulse delivered at the onset of the traces).

Use of square voltage calibration pulses as a reference for deconvolution of the physiological signals

The shape and amplitude of the signals recorded by the gMμEs differ from those recorded by the DC coupled intra-

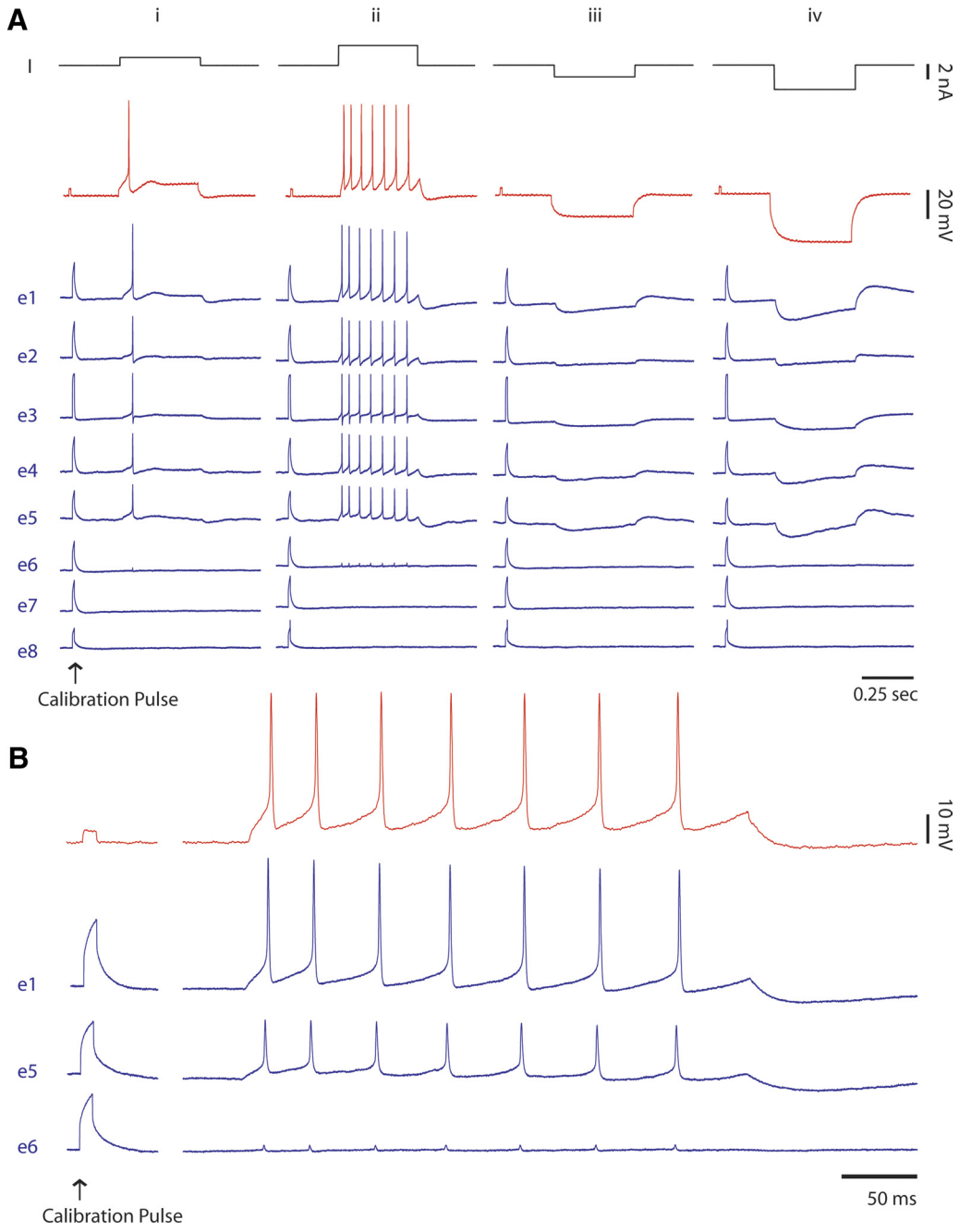

FIG. 2. In-cell recording of action potentials and subthreshold hyperpolarizing pulses by gMμEs. A neuron was cultured for 2 days on a gMμEs based device. Recordings of action potentials and hyperpolarizing pulses generated by an intracellular glass microelectrode inserted into the soma were made from 8 gMμEs. Six gMμEs reside under the neuron (*e1–e6*) and 2 away from it (*e7* and *e8*). *A*: a 5 mV, 10 ms square calibration pulse is delivered at the onset of each voltage trace (red and blue). Depolarizing current pulses injected through the intracellular electrode (*A, I* and *ii,* black) generated membrane depolarization that reached threshold to fire a single action potential (*i,* red) and a train of action potentials (*ii,* red). These action potentials were recorded by gMμE *e1–e6* (*i* and *ii,* blue). The trace showing the trains of action potentials recorded by the intracellular electrode (*ii,* red) and gMμEs *e1*, *e5,* and *e6* (*ii,* blue) are enlarged in *B*. Note the differences in the shapes and amplitude of the 5 mV 10 ms calibration pulses and the action potentials. In *columns iii* and *iv*, hyperpolarizing square pulses were delivered by the intracellular glass microelectrode (black). Note the different degrees of electrical coupling between the neuron and the gMμEs and the differences in the filtering of the DC pulse by the different gMμEs (*ii* and *iv,* red and blue).

cellular sharp electrode. The differences in the shape of the signals are attributed to the transfer properties of the electrical impedance generated by the ionic bilayer formed at the interface between the gMμE and the culture medium (Mortari et al. 2007) and of the AC amplifier used. The attenuation in the amplitude is further attributed to the quality of the seal resistance formed between the plasma membrane and the gMμE and the conductance of the patch of plasma membrane that faces the gMμE (Fig. 3 and discussed in the following text). Because the parameters that represent individual neuron-gMμE junction are not identical, the alterations in the signal shape and attenuation factor differ for individual gMμEs. Nevertheless these individual alterations can be corrected using the calibration pulse as a reference.

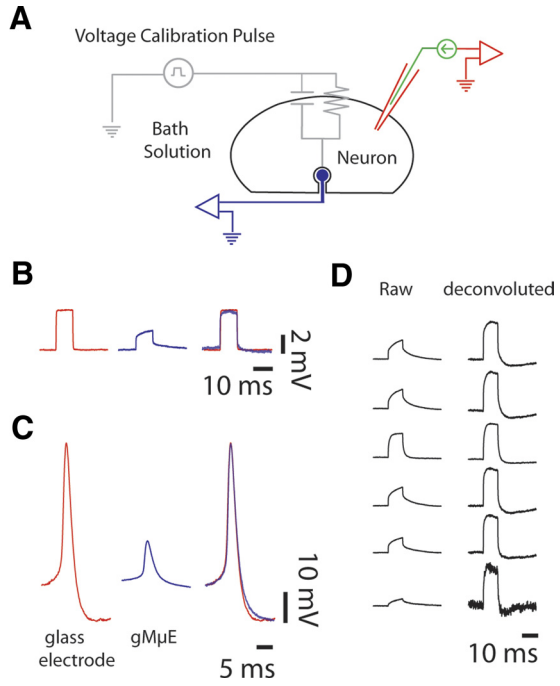

FIG. 3. *A*: experimental setup. Deconvolution of the signals recorded by the gMμEs. The known shape and amplitude of the calibration pulse is used to deconvolute the potentials recorded by the gMμEs. *B*: in red, the 5 mV, 10 ms calibration pulse as recorded by the DC coupled intracellular glass microelectrode. In blue, the same calibration pulse as recorded by an AC coupled gMμE. Superpositioning of the deconvoluted AC coupled calibration pulse and the DC coupled calibration reveals a reasonable fit. *C*: deconvolution of the action potential recorded by the same electrode as in *A*. Intracellular recorded action potential (red), the same action potential as recorded by the gMμEs (blue). After deconvolution using the same parameters used in *A*, super positioning of the spikes reveals a reasonable fit. *D*: examples of the impedance distortion introduced by different electrodes (left hand side), each altering the calibration pulse in accordance to the gMμE electrical characteristics and its deconvoluted form (right hand side). (Note: deconvolution was performed using an off-line negative capacitance circuit, see text for details).

We began to apply a correction protocol using as a reference the known amplitude and shape of the voltage calibration square pulse. The calibration pulse was applied through the reference Ag/AgCl electrode using an isolated calibration pulse generator (Fig. 3*A*). At the onset of each trace, a 5 mV, 10 ms calibration square pulse was delivered to the bathing solution and recorded by the DC-coupled sharp glass electrode (Figs. 2 and 3*B*, red) and simultaneously recorded by the individual AC coupled gMμEs (Figs. 2 and 3*B*, blue). Using a standard off-line negative capacitance compensation circuit (McGillivray and Wald 1980; Wilson and Park 1989), the gMμE-distorted calibration pulse was partially corrected (Fig. 3*B*, *right*, a deconvoluted signal is shown in blue and is superimposed on the original calibration pulse, shown in red). We next applied the same negative capacitance parameters to the action potentials recorded by the gMμE (Fig. 3*C*). Superposition of the DC coupled intracellularly recorded action potential (Fig. 3*C*, red) and the deconvoluted gMμE -recorded action potential (*C*, blue) reveals good match in both shapes and amplitudes. Using this approach, it was not possible to deconvolute the long-duration pulses due to the low-frequency filtering of the AC-coupled amplifier used.

In-cell recording of subthreshold synaptic events

To further illustrate the quality of the recording provided by the gMμE based microelectrode array, we cocultured homologous *Aplysia* neurons that form electrical synapses (Benbassat and Spira 1994; Carrow and Levitan 1989; Rayport and Schacher 1986). Figure 4 depicts an experiment performed on two neurons cultured on a gMμE array for 2 days. For the experiment, a sharp glass microelectrode, for both current injection and voltage recording, was inserted to *neuron 1,* and recordings were made with a gMμE from *neuron 2* (Fig. 4*A*). Hyperpolarizing square current pulse delivered to *neuron 1,* generated membrane hyperpolarization of *neurons 1* and *2* (Fig. 4*B*). The coupling coefficient (the algebraic scaling factor) between *neuron 1* (as recorded by an intracellular DC coupled electrode) and the raw signal recorded in *neuron 2* (by the AC coupled gMμE, Fig. 4*B*, *iii*) was estimated to be 0.2–0.3. Consistent with these observations, firing of *neuron 1* (Fig. 4*C, ii,* red) generated an excitatory postsynaptic potential (EPSP) in *neuron 2* (Fig. 4*C, iii,* blue) which reached threshold to initiate an AP (Fig. 4*C, iii*). The AP in *neuron 2* (Fig. 4*C, iii*) in turn initiated an excitatory postsynaptic potential (EPSP) in *neuron 1* (Fig. 4*C, ii*). Trains of action potentials generated by the intracellular electrode in *neuron 1* (Fig. 4*C, right*) generated a train of EPSPs in *neuron 2* that summated to fire a train of action potentials (Fig. 4*C, iii right*).

Thus in spite of the filtering and attenuation of the signals by the gMμE impedance and AC coupled amplifier, the quality of recording by the extracellular positioned gMμE is of unprecedented quality. It is important to recall that as a consequence

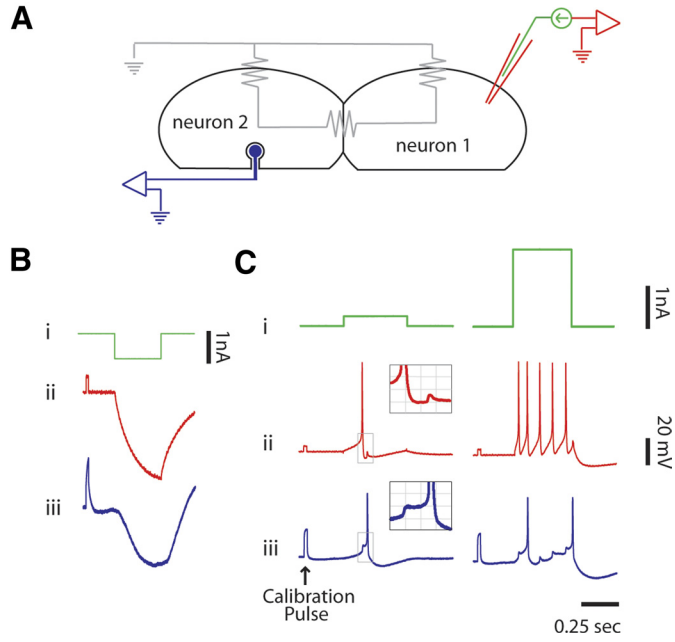

FIG. 4. In-cell recording of subthreshold synaptic potentials. *A*: experimental setup. *B*: hyperpolarizing square current pulse shown in green delivered to *cell 1* (right hand side in *A*), generated membrane hyperpolarization of both *cells 1* and *2* (*B, ii* and *iii*) demonstrating the electrical coupling between the cells. *C*: depolarizing square current pulse shown in green (*i*) delivered to *cell 1* elicited firing of an action potential (*C, ii*) and generated an excitatory postsynaptic potential (EPSP) in *cell 2* (*C, iii*). The AP in *cell 2* (*C, iii*) in turn initiated an EPSP in *cell 1* (*C, ii; insets*: closeup of concurrently recorded EPSPs and APs in both cells). Trains of action potentials (*right panels*) generated by the intracellular electrode in *cell 1*generated a train of EPSPs in *cell 2* (*iii*) that summated to fire a train of action potentials.

of the specific impedance of any given gMμE within an array and its coupling level with the neuron, its filtering of the amplitude and shape of a recorded signal will differ (see Fig. 3 and accompanying discussion).

Stability of the gMμE-neuron junction

A critical feature of the extensive use of extracellular recording for in vitro and in vivo research purposes as well as for potential future clinical applications is the noninvasive nature of the electrodes that permits long term recordings. In an earlier study, we established that culturing *Aplysia* neurons on a dense matrix (4, 8, 12, and 16 μm pitch) of gold mushroom-shaped protrusions for over a week does not alter the excitable membrane properties and synaptic physiology of the neurons (Hai et al. 2009b). However, we did not examine the functional stability of the junctions formed between the neurons and the gMμE. Here we began to examine this question by culturing spontaneously active *Aplysia* neurons on gMμE-based microelectrode arrays (Fig. 5). We found that effective electrical coupling between neurons and gMμEs was maintained for >48 h (the longest period of time that we so far attempted to follow, Fig. 5*A*). It should be noted that in these experiments the shape and amplitude of the action potentials over this period were not absolutely stable. The mechanism underlying the variability was not analyzed yet as at this early stage of the investigations (given the constraints of limited availability of chips), we avoided the risk of cultures contamination by not taking off the cover from the culture dish for insertion of a conventional sharp intracellular microelectrode for comparison. A number of mechanisms could account for the observed changes. These include: small alterations in the neurons resting potential, changes in the junctional membrane resistance or seal resistance (see DISCUSSION of the analog electrical circuit in the following text). To the best of our knowledge, such recording sessions with lengths of over 2 days were never conducted.

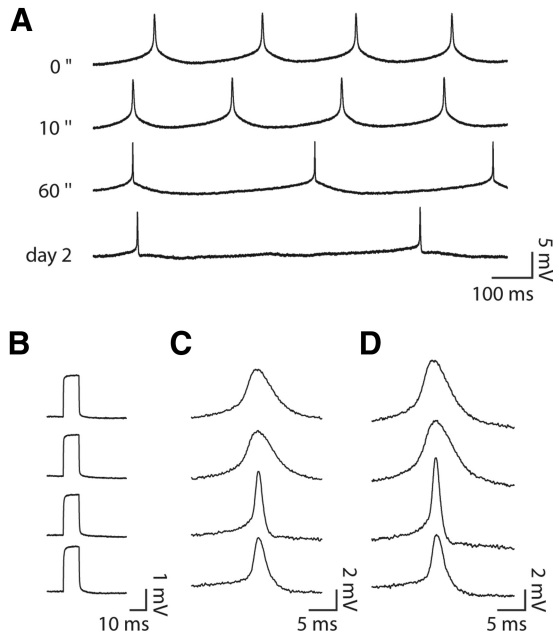

FIG. 5. Long term in-cell recording from a spontaneously active neuron. *A*: recording sessions from the same neuron of hours and days are maintained (time is given on the left). *B*: calibration pulse along 2 days of recordings. *C*: the shapes and amplitudes of the raw action potentials recorded by gMμEs along 2 days. *D*: deconvolution of the recorded action potentials.

Stimulation of neurons by gMμE

Analysis of neuronal circuits largely relies on repeated use of stimulating electrodes. It is of critical importance that stimuli are delivered without damaging the cells (Schoen and Fromherz 2008). Whereas current injection (stimulation) by intracellular sharp glass electrodes or patch electrodes involves no difficulty, stimulation by extracellular high-impedance electrodes is complicated by the relatively limited charge transfer to the plasma membrane, by the risk of damaging the cells by electroporation (He et al. 2007; Rubinsky 2007; Ryttsen et al. 2000), or by irreversible electrochemical reaction products (Brummer et al. 1983; Harnack et al. 2004; Merrill et al. 2005; Yao et al. 2001). To overcome these problems, trains of weak capacitive stimuli can be delivered to cultured cells to activate local sodium currents that generate sufficient depolarization to reach firing threshold (Schoen and Fromherz 2008). While this approach is safe, it might complicate experimental protocols in which precisely timed consecutive stimuli are to be delivered.

Here we began to examine whether the interface formed between the gMμEs and the neurons as well as the gMμE properties support effective stimulation of the neurons without inducing irreversible electroporation. To that end, a neuron cultured on a gMμE based microelectrode array was impaled by a sharp electrode for both current injection and voltage recordings (Fig. 6, red). We next characterized the coupling level between the neuron and the gMμE and selected to concentrate on two gMμEs, one with high coupling and the other with low coupling values gMμE1 and gMμE2, respectively; Fig. 6*B, i* blue). Hyperpolarization of the neuron by current injection through the intracellular electrode leads to hyperpolarization of gMμE-1 and to a much smaller extent gMμE-2 (Fig. 6*B, i*). Consistently, depolarization of the neuron to fire an action potential leads to the generation of an action potential of ~3 mV recorded by gMμE-1 and ~0.5 mV by gMμE −2 (Fig. 6, *Ci* and *Di,* respectively). Delivering a single depolarization square voltage step of 1–10 ms, with an increasing voltage from 1,400 to 1,800 mV by gMμE-1 evoked depolarization of the neuron that reached threshold to fire action potentials as recorded by the glass microelectrode (Fig. 6*E, top*). Applying similar current pulses to gMμE-2 depolarized the neuron but failed to reach threshold (Fig. 6*E, bottom*).

To examine whether this series of stimulations (5–10 stimulations per experiment) via the gMμE induced damages to the neuron, we once again delivered hyperpolarizing pulses through the intracellular glass microelectrode and measured the input resistance and the coupling between the neurons and the gMμEs. As evidenced in Fig. 6 (*Bii, Cii,* and *Dii*), the stimuli delivered by the gMμE did not induce detectable changes to the neuron's input resistance or altered the coupling coefficient between the neuron and the gMμE.

We conclude that provided that the coupling coefficient is good, the in-cell configuration enables to inject sufficient current to reach firing threshold of the neuron without inflicting damages to the plasma membrane or the junction.

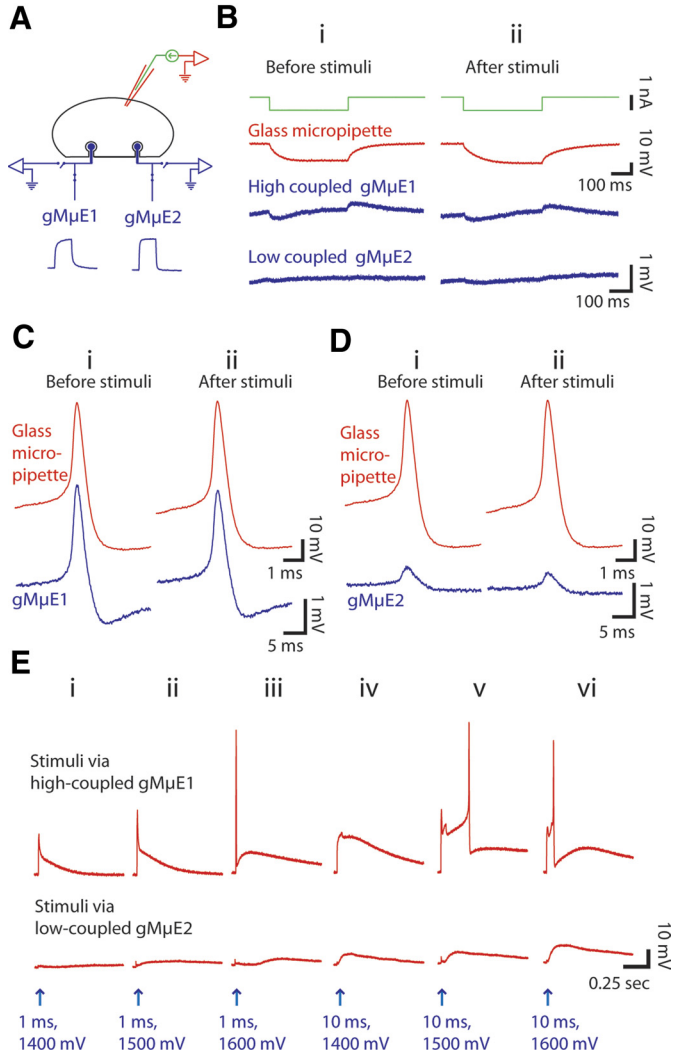

FIG. 6. Stimulation by gMμEs without damage to the cell. *A*: experimental setup. *B*: hyperpolarizing square current pulse (green traces) delivered to the cell by the glass intracellular electrode generated membrane hyperpolarization (red traces) detected by both high and low coupled gMμEs (gMμE1 and gMμE2, respectively, blue traces *Bi*). The input resistance and level of coupling between the neuron and gMμE1 and gMμE2 is not changed before and after the application of stimuli delivered by gMμE1 and gMμE2 stimulation (shown in *E*). *C* and *D*: action potential shape, duration, and amplitude as recorded by gMμE1 and gMμE2. These are not changed by the use of gMμE1 and gMμE2 to stimulate the neuron (shown in *E*). *E*: stimulation of the neuron by gMμE1 and gMμE2 while recording with the intracellular glass microelectrode. The strength of the applied stimulus and its duration are given below the traces. Note that whereas the high coupled gMμE1 (*top*) generated an action potential, the low coupled gMμE2 did not reach threshold.

Analog electrical equivalent circuit of the neuron-gMμE interface for recording and stimulation

The unprecedented electrical coupling between neurons and engulfed gMμEs is analyzed in the following paragraphs by the use of the analog electrical *equivalent* circuit shown in Fig. 7. The model includes a neuron composed of a nonjunctional membrane characterized by a passive RC circuit with parameters (R_{nj}; C_{nj}) and a junctional membrane facing the gMμE (R_j; C_j). The cleft formed between the neuron's plasma membrane and the surface of the gMμE (R_{seal}) and the gMμE ($R_{gM\mu E}$ and $C_{gM\mu E}$). The majority of parameters used for the simulation were obtained from direct measurements or by calculations of the physical parameters that fit the specific geometry of the gMμE and the neuron-gMμE interface (see experimental procedures). The expected coupling coefficient for action potentials (high frequencies of 100–1,000 Hz) and long (DC) pulses were calculated as a function of R_{seal} using different values for the junctional membrane resistance (ranging from 10 MΩ to 100 GΩ; Fig. 7, *B* and *C*). Based on ultrastructural information, we evaluated in an earlier study the expected values of R_{seal} to be 67 MΩ (Hai et al. 2009a).

Based on this parameter (R_{seal} ~100 MΩ), we evaluated the range of possible values of the junctional membrane conductance, which generate the experimentally observed coupling coefficient (i.e., 0.05–0.5) to be 10–100 MΩ.

Assuming that the junctional membrane conductance is increased by recruitment of voltage independent ionic channels such as potassium channels with single channel conductance of 10 to 100 pS, then ~10–100 such channels have to concentrate within the confined area of the junctional membrane. This would imply a density of ~0.5–10 channels/μm^2. This density is physiological and was documented in many cell types (Hille 2001).

It is important to recall that the coupling between the neurons and the gMμE depends on the value of the seal resistance. Reducing the seal resistance to values <100 MΩ reduces the coupling coefficient drastically (Fig. 7, *B* and *C*).

Using the same values, we next simulated the experiments of Fig. 6*E*, modeling the membrane depolarization induced by the delivery of a millisecond long voltage pulse delivered by a gMμE. Figure 7*D* depicts the membrane depolarization induced by such a pulse assuming that g_j = 100 MΩ, R_{seal} = 100 MΩ, and gMμE capacitance is either low (5 pF) or high (40 pF). We have found that for high capacitance gMμE a ~1,500 mV voltage results in a maximum depolarization of ~35 mV, which is sufficient to elicit an action potential (as is the case shown in Fig. 6*E*).

DISCUSSION

The present study demonstrated that neuron-gMμE interface forms an unexpected junction that supports high quality bidirectional electrical coupling. This configuration enables in-cell recording with quality and signal-to-noise ratio that matches classical sharp- and patch- electrode intracellular recording. The interface also supports "in-cell-stimulation" by milliseconds long single pulses. Consistent with the extracellular position of the gMμEs in respect to the neurons, the recording sessions could last for >2 days (the longest time that we followed spontaneous firing activities) and most likely for significantly longer periods. The physical principles underlying the in-cell recording and stimulation are similar to those of the perforated patch clamp configuration (Akaike and Harata 1994; Inyushin et al. 1997). The novel approach that we present here differs from the prevailing methodologies of intracellular recordings or patch clamping mainly in that rather than to use our "muscles" to push the electrode into contact with the cells and break its membrane, we "persuade" the cells to use their own muscles to "swallow the bait-microelectrodes" and thus bring the cell and the microelectrode into the needed level of physical intimacy.

Three essential components converge to generate the in-cell interface configuration: physical, chemical and biological. In

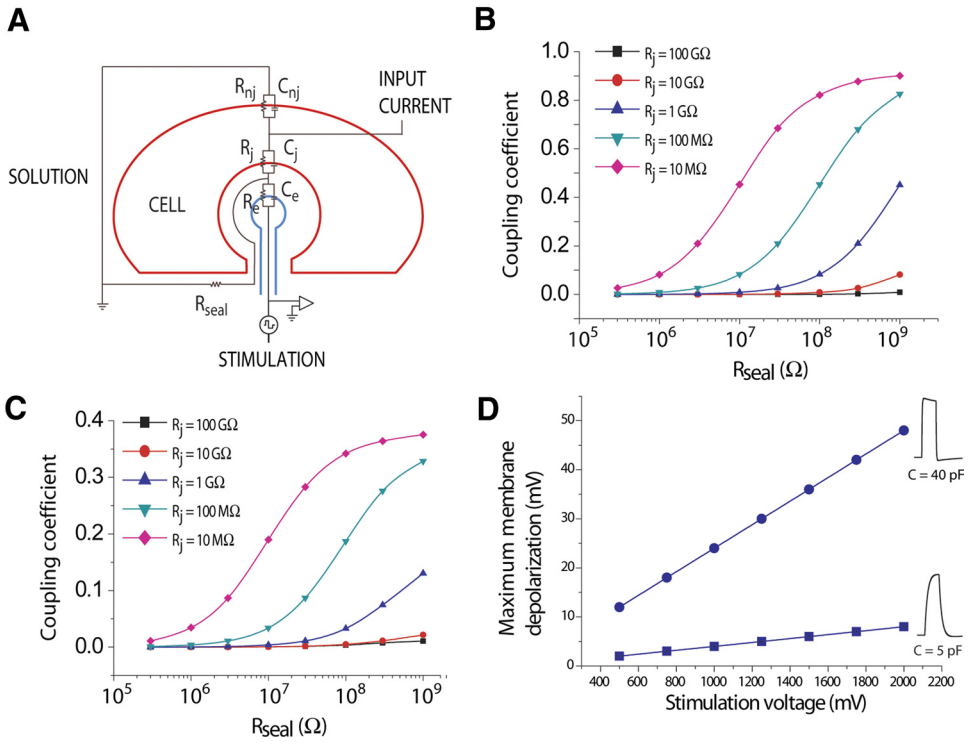

FIG. 7. Electrical model representing the gMμE-neuron junction. *A*: equivalent circuit of gMμE-neuron junction. *B* and *C*: coupling coefficient as a function of seal resistance and the resistance of the junctional membrane in high-frequency (100 Hz; *B*) and low frequency (1 Hz; *C*) signals. *D*: maximum membrane depolarization as a function of amplitude of voltage-based stimulation through the gMμE in high (●) and low (■) capacitance gMμEs. Application of a ~1,500 mV voltage results in a maximum depolarization of ~35 mV, which is sufficient to elicit an action potential.

the following text, we first discuss the physical principles that underlie the in-cell junctional configuration and then discuss our current understanding of the contribution of each one of its components.

Physical principles underlying the in-cell recording and stimulation configuration

Two earlier studies by Jenkner and Fromherz (1997) and Cohen et al. (2008) paved the conceptual approach to the development of the method. Both studies illustrated that the transient mechanical downward displacement of leech or *Aplysia* neurons cultured over a flat transistor gate leads to increase in the R_{seal} and was also associated with an increase in g_j. The increased R_{seal}, in concert with the increased g_j, led to transformation of a low-amplitude biphasic extracellular field potential (FP), which is proportional to the first derivative of the intracellular voltage, to a monophasic FP which resembles in shape intracellularly recorded action potentials. In the pioneering studies of Fromherz laboratory, they referred to such monophasic potential as a B-spike (Fromherz 2003). In the case of *Aplysia* neurons, the amplitudes of such potential reached values of 30 mV. Whereas these studies demonstrated in principle a method to significantly improve the signal to noise and create conditions to generate semi-intracellularly recorded action potentials from cultured neurons, the method of neuron mechanical compression against the substrate could not be considered for routine experimental applications. Interestingly, recent studies also revealed occasional positive extracellular 1 mV high action potentials when extracellular electrodes were introduced into cat visual cortex under in vivo conditions (Blanche et al. 2005; Gold et al. 2009). Attempts to explain the mechanisms underlying the generation of these positive spikes were so far incomplete (Gold et al. 2009). In view of the findings of Jenkner and Fromherz (1997), Cohen et al. (2008), Hai et al. (2010), and the present study, it would be interesting to consider the possibility that occasionally insertion of an extracellular electrode generates a semi-stable in-cell-like junction.

Geometry and surface chemistry of the gMμE

The two cell biological principles that are involved in the process of in-cell interface formation are: active engulfment of the chemically functionalized gMμEs by the neurons and the generation of high seal resistance and the recruitment or activation of ion channels within the patch of the plasma-membrane that faces the gMμE - the junctional membrane (Fig. 1). We have not studied the mechanisms underlying the generation of these critical events but noted in an earlier structural study (Hai et al. 2009b) that engulfment of gMμEs is much more effective when functionalized with EPP than by poly-L-lysine. We thus tentatively believe that the EPP plays a role in the induction of the engulfment and that binding events of receptors displayed on the plasma membrane and the EPP activate a highly conserved cascade leading to phagocytosis like processes (Stuart and Ezekowitz 2005). The mechanism by which the neurons elevate the conductance of the plasma membrane facing the gMμEs and generate the assembly of actin ring around the stalk of the gMμEs may be related to the geometry of the gMμEs (Hai et al. 2009b). Two mechanisms are proposed in the literature that could account for the localized increase in the junctional membrane conductance predicted from the model. Both are related to the geometry of the substrate. In the first mechanism, convex surface causes BAR-domain protein (bin, amphiphysin, Rvs domain) to release Rac (a GTPase), which in turn leads to local cytoskeleton rearrangements. This in turn may result in redistribution of ion channels. The second mechanism is that membrane curvature alters the mechanical tension on the inner and outer faces of the

lipid bilayer and thereby activate ion channels or increase the local conductance (for review, Vogel and Sheetz 2006). Better understanding of these parameters may in the future improve the design of the chemistry and geometry of the protruding microelectrodes leading to better electrical interface.

Application of the in-cell recording and stimulation to mammalian neurons

Under the specific experimental conditions used in the current study, the plating of isolated *Aplysia* neurons directly on top of the functionalized gMμE leads to optimal positioning of the neurons in respect to the gMμE and their engulfment. Live confocal microscope imaging revealed that within 10–20 min of contact actin rings assemble around the gMμEs stalk (Hai et al. 2009b). The actin rings become a stable cytoskeleton structures and are maintained for $\geq$10 days (the longest period that we examined it).

Ultrastructural observations revealed that other cell types such as CHO, 3T3, H9C2 and PC12 cell lines cultured on a matrix of gMμEs functionalized by the EPP also engulfs the gMμEs (Hai et al. 2009a). We wish to note though that these observations do not necessarily imply that primary mammalian neurons or other cell types will respond in a similar way.

Future attempts to apply the in-cell recording and stimulation configuration to smaller mammalian neurons will require generating culture conditions that will lead the neurons to optimally self-position themselves in respect to the gMμEs and to functionalize the gMμEs by proper signaling molecules to induce gMμE engulfment (phagocytosis). In addition, these events must be associated with elevation of the conductance of the patch of membrane that faces the gMμE. The above-described steps are expected to generate the necessary physical conditions to generate an effective interface. Additional obstacles in assembly of the junctions are expected. The most prominent one is the competition of glia cells over the engulfment of the gMμE thus preventing neurons from forming close physical apposition with the gMμE.

ACKNOWLEDGMENTS

The fabrication of the gold spines electrode was carried at the Harvey M. Kruger Family Center for Nanoscience and Nanotechnology. We thank N. Mazurski for expertise in device fabrication, R. Rosenbaum for helpful comments regarding analysis of data. M. E. Spira is the Levi DeViali Professor in neurobiology.

GRANTS

Supported by the "Brain Storm" project (EU P7 215486 STREP). Parts of the study were carried out at the Charles E. Smith and Prof. Elkes Laboratory for Collaborative Research in Psychobiology. A. Hai was supported by a scholarship from The Israel Council for Higher Education.

DISCLOSURES

No conflicts of interest, financial or otherwise, are declared by the author(s).

REFERENCES

Akaike N, Harata N. Nystatin perforated patch recording and its applications to analyses of intracellular mechanisms. *Jpn J Physiol* 44: 433–473, 1994.

Ashery U, Penner R, Spira ME. Acceleration of membrane recycling by axotomy of cultured *Aplysia* neurons. *Neuron* 16: 641–651, 1996.

Bailey CH, Kandel ER. Synaptic remodeling, synaptic growth and the storage of long-term memory in *Aplysia*. *Prog Brain Res* 169: 179–198, 2008.

Benbassat D, Spira ME. The survival of transected axonal segments of cultured *Aplysia* neurons is prolonged by contact with intact nerve-cells. *Eur J Neurosci* 6: 1605–1614, 1994.

Berdondini L, Massobrio P, Chiappalone M, Tedesco M, Imfeld K, Maccione A, Gandolfo M, Koudelka-Hep M, Martinoia S. Extracellular recordings from locally dense microelectrode arrays coupled to dissociated cortical cultures. *J Neurosci Methods* 177: 386–396, 2009.

Berger TK, Perin R, Silberberg G, Markram H. Frequency-dependent disynaptic inhibition in the pyramidal network: a ubiquitous pathway in the developing rat neocortex. *J Physiol* 587: 5411–5425, 2009.

Blanche TJ, Spacek MA, Hetke JF, Swindale NV. Polytrodes: high-density silicon electrode arrays for large-scale multiunit recording. *J Neurophysiol* 93: 2987–3000, 2005.

Brummer SB, Robblee LS, Hambrecht FT. Criteria for selecting electrodes for electrical stimulation: theoretical and practical considerations. *Ann NY Acad Sci* 405: 159–171, 1983.

Carrow GM, Levitan IB. Selective formation and modulation of electrical synapses between cultured *Aplysia* neurons. *J Neurosci* 9: 3657–3664, 1989.

Cohen A, Shappir J, Yitzchaik S, Spira ME. Reversible transition of extracellular field potential recordings to intracellular recordings of action potentials generated by neurons grown on transistors. *Biosens Bioelectron* 23: 811–819, 2008.

Fee MS, Mitra PP, Kleinfeld D. Automatic sorting of multiple unit neuronal signals in the presence of anisotropic and non-Gaussian variability. *J Neurosci Methods* 69: 175–188, 1996.

Fromherz P. *Neuroelectronic Interfacing: Semiconductor Chips With Ion Channels, Nerve Cells, and Brain.* Berlin: Wiley-VCH, 2003.

Fromherz P. Three levels of neuroelectronic interfacing: silicon chips with ion channels, nerve cells, and brain tissue. *Ann NY Acad Sci* 1093: 143–160, 2006.

Fromherz P, Offenhausser A, Vetter T, Weis J. A neuron-silicon junction: a Retzius cell of the leech on an insulated-gate field-effect transistor. *Science* 252: 1290–1293, 1991.

Gold C, Girardin CC, Martin KA, Koch C. High-amplitude positive spikes recorded extracellularly in cat visual cortex. *J Neurophysiol* 102: 3340–3351, 2009.

Hai A, Dormann A, Shappir J, Yitzchaik S, Bartic C, Borghs G, Langedijk JP, Spira ME. Spine-shaped gold protrusions improve the adherence and electrical coupling of neurons with the surface of micro-electronic devices. *J R Soc Interface* 6: 1153–1165, 2009a.

Hai A, Kamber D, Malkinson G, Erez H, Mazurski N, Shappir J, Spira ME. Changing gears from chemical adhesion of cells to flat substrata toward engulfment of micro-protrusions by active mechanisms. *J Neural Eng* 6:66009, 2009b.

Hai A, Shappir J, Spira ME. In-cell recordings by extracellular microelectrodes. *Nat Methods* 7: 200–202, 2010.

Harnack D, Winter C, Meissner W, Reum T, Kupsch A, Morgenstern R. The effects of electrode material, charge density and stimulation duration on the safety of high-frequency stimulation of the subthalamic nucleus in rats. *J Neurosci Methods* 138: 207–216, 2004.

He H, Chang DC, Lee YK. Using a micro electroporation chip to determine the optimal physical parameters in the uptake of biomolecules in HeLa cells. *Bioelectrochemistry* 70: 363–368, 2007.

Hille B. *Ion Channels of Excitable Membranes*. Sunderland, Mass: Sinauer, 2001.

Hochberg LR, Serruya MD, Friehs GM, Mukand JA, Saleh M, Caplan AH, Branner A, Chen D, Penn RD, Donoghue JP. Neuronal ensemble control of prosthetic devices by a human with tetraplegia. *Nature* 442: 164–171, 2006.

Hutzler M, Lambacher A, Eversmann B, Jenkner M, Thewes R, Fromherz P. High-resolution multitransistor array recording of electrical field potentials in cultured brain slices. *J Neurophysiol* 96: 1638–1645, 2006.

Inyushin M, Tsytsarev V, Ignashchenkova A, Lenkov DN. Use of artificial ion channels for quasi-intracellular recording of cerebral cortex neuron activity. *Neurosci Behav Physiol* 27: 702–707, 1997.

Jenkner M, Fromherz P. Bistability of membrane conductance in cell adhesion observed in a neuron transistor. *Phys Rev Lett* 79: 4705–4708, 1997.

Le Be JV, Markram H. Spontaneous and evoked synaptic rewiring in the neonatal neocortex. *Proc Natl Acad Sci USA* 103: 13214–13219, 2006.

McAdams ET, Jossinet J, Subramanian R, McCauley RG. Characterization of gold electrodes in phosphate buffered saline solution by impedance and noise measurements for biological applications. *Conf Proc IEEE Eng Med Biol Soc* 1: 4594–4597, 2006.

McGillivray R, Wald R. Dual-path capacitance compensation network for microelectrode recordings. *Am J Physiol Heart Circ Physiol* 238: H930–931, 1980.

Merrill DR, Bikson M, Jefferys JG. Electrical stimulation of excitable tissue: design of efficacious and safe protocols. *J Neurosci Methods* 141: 171–198, 2005.

Mirsky VM, Riepl M, Wolfbeis OS. Capacitive monitoring of protein immobilization and antigen-antibody reactions on monomolecular alkylthiol films on gold electrodes. *Biosens Bioelectron* 12: 977–989, 1997.

Mortari A, Maaroof A, Martin D, Cortie MB. Mesoporous gold electrodes for sensors based on electrochemical double layer capacitance. *Sensors and Actuators B Chem* 123: 262–268, 2007.

Neves G, Cooke SF, Bliss TV. Synaptic plasticity, memory and the hippocampus: a neural network approach to causality. *Nat Rev Neurosci* 9: 65–75, 2008.

Rayport SG, Schacher S. Synaptic plasticity in vitro: cell culture of identified *Aplysia* neurons mediating short-term habituation and sensitization. *J Neurosci* 6: 759–763, 1986.

Rubehn B, Bosman C, Oostenveld R, Fries P, Stieglitz T. A MEMS-based flexible multichannel ECoG-electrode array. *J Neural Eng* 6: 036003, 2009.

Rubinsky B. Irreversible electroporation in medicine. *Technol Cancer Res Treat* 6: 255–260, 2007.

Ryttsen F, Farre C, Brennan C, Weber SG, Nolkrantz K, Jardemark K, Chiu DT, Orwar O. Characterization of single-cell electroporation by using patch-clamp and fluorescence microscopy. *Biophys J* 79: 1993–2001, 2000.

Sakmann B, Neher E. Patch clamp techniques for studying ionic channels in excitable membranes. *Annu Rev Physiol* 46: 455–472, 1984.

Schoen I, Fromherz P. Extracellular stimulation of mammalian neurons through repetitive activation of Na^+ channels by weak capacitive currents on a silicon chip. *J Neurophysiol* 100: 346–357, 2008.

Shahaf G, Eytan D, Gal A, Kermany E, Lyakhov V, Zrenner C, Marom S. Order-based representation in random networks of cortical neurons. *PLoS Comput Biol* 4: e1000228, 2008.

Shoham S, Fellows MR, Normann RA. Robust, automatic spike sorting using mixtures of multivariate t-distributions. *J Neurosci Methods* 127: 111–122, 2003.

Spira ME, Dormann A, Ashery U, Gabso M, Gitler D, Benbassat D, Oren R, Ziv NE. Use of *Aplysia* neurons for the study of cellular alterations and the resealing of transected axons in vitro. *J Neurosci Methods* 69: 91–102, 1996.

Spira ME, Kamber D, Dormann A, Cohen A, Bartic C, Borghs G, Langedijk JPM, Yitzchaik S, Shabthai K, Shappir J. Improved neuronal adhesion to the surface of electronic device by engulfment of protruding micro-nails fabricated on the chip surface. *Transducers '07 Eurosensors Xxi, Digest Techn Papers* 1: 1247–1250, 2007.

Stuart LM, Ezekowitz RA. Phagocytosis: elegant complexity. *Immunity* 22: 539–550, 2005.

Wilson CJ, Park MR. Capacitance compensation and bridge balance adjustment in intracellular recording from dendritic neurons. *J Neurosci Methods* 27: 51–75, 1989.

Yao Y, Zhang D, Luo Y, Huang A, Zhou W, Ren H. Influence of electroporation on the biological activities of primary rat hepatocytes. *Zhonghua Gan Zang Bing Za Zhi* 9: 178–180, 2001.

Cover:

Neurons growing on a matrix of gold-mushroom microelectrodes. Illustration concept by Aviad Hai, computer generated model by Ariel Chai. For details see Hai A, Shappir J, and Spira ME. Long-Term, Multisite, Parallel, In-Cell Recording and Stimulation by an Array of Extracellular Microelectrodes. J Neurophysiol 104: 559–568, 2010; first published April 28, 2010; doi:10.1152/jn.00265.2010.